

Photoemission from adsorbate-covered Ag films: The dispersion relation for Ag plasma excitation

T. H. Koschmieder and J. C. Thompson

Department of Physics, The University of Texas at Austin, Austin, Texas 78712

(Received 6 June 1994)

We have studied photoemission from an adsorbate-covered Ag film in an attenuated-total-reflection configuration and with direct illumination of the film. From the peaks in the photoemission as a function of angle of incidence of the light, $P(\vartheta)$, we have determined the dispersion relation for the excitation responsible for the peaks. There are three branches. The dispersion curve for the photoemission below 3.6 eV is the same as that for surface plasmon-polariton excitation. In the range between the surface and bulk plasmon limits, 3.6–3.8 eV, the dispersion curve bends backwards, i.e., with increased energy the angle for peak photoyield decreases. The third branch to the dispersion curve is above 3.8 eV and the peak photoyield occurs at increasing angle with increasing energy E . Large photoyield in both the second and third regimes requires a large imaginary part of the dielectric constant. The dispersion curve $E(\vartheta)$ and the shape of $P(\vartheta, E)$ agree with a calculation based on a model of Pepper [J. Opt. Soc. Am. **60**, 805 (1970)]. We have found the temperature coefficient of the minimum in $P(E)$ at $\varepsilon_2(\omega)=0$ to be -2.5×10^{-4} eV/K.

I. INTRODUCTION

The geometry of an attenuated-total-reflection (ATR) experiment is designed¹ to enhance coupling to a surface plasmon polariton (SPP). The decay of a SPP is often into a single electron that is then a candidate for photoemission. In the present experiment we have used the ATR geometry and an adsorbate-covered Ag film to study photoemission in the energy range of the bulk (3.80) and surface (3.65 eV) plasmons and the interband transition responsible for the unique optical properties of Ag. In addition, we have studied photoemission with direct illumination of the Ag film through the adsorbate monolayer. In contrast to some previous work,^{2–4} we have used a UHV system allowing for careful control of film morphology and adsorbate coverage.

The adsorbate, 4-picoline (4-methyl pyridine), lowers the work function from ≈ 4.35 to 2.6 eV in a manner similar^{5–7} to Cs and without any appreciable effect on the optical properties of Ag.

There have been several studies of photoemission from Ag (Refs. 3, 4, 8, and 9) and Al (Refs. 2, 5, 8, and 10) surfaces, some with cesiation.^{5–7} Most have been in much less well-characterized systems and over much narrower energy ranges than the present work.

Our measurements include the reflectance R and photoyield P as functions of angle ϑ at a fixed photon energy, $2 < E < 5$ eV, and also R and P as functions of energy at fixed angle. Measurements were made for light directly incident on the exposed surface of the metal film as well as through the ATR prism. The result is composites of $R(\vartheta, E)$ and $P(\vartheta, E)$. We can thus follow the dispersion curve $E(\vartheta,)$ for photoemission resonant at the angle $\vartheta,$ to the intermediate regime between surface and bulk plasmon excitation, and into the range above the bulk plasma frequency.

We interpret our observations in terms of a model proposed by Pepper¹¹ and used already by others^{2,5} for

volume photoemission in an ATR system. Pepper¹¹ computes the energy adsorbed at a given depth in a thin film from the Poynting vector and integrates over the escape length. The theory provides a satisfactory description of the usual, linear photoemission in ATR experiments above threshold.^{2,5}

II. EXPERIMENT

A hemicylindrical fused silica prism is used as the substrate for the experiment. The prism is coated on one half of the circular side with an Al film¹² and the cylinder ends are clamped between two Cu blocks. A Cu band in the cold finger is used with Cu braids to connect the liquid-N₂-filled cold finger to the Cu prism mount. Cooling yields temperatures of about 150 K.

The prism is rotated in the vacuum chamber by a Varian UHV rotation feedthrough that is concentric with the cold finger but separate. Rotation is controlled by a UNIDEX II motion controller. Obviously the Cu braids do not allow infinite rotation.

The experiments were made in a UHV system with a base pressure of 5×10^{-10} Torr. Ag is deposited *in situ*. During evaporations the pressure would rise into the high 10^{-9} -Torr range. The Ag source is located so that the flat prism surface can be rotated to be perpendicular to the Ag atom path. Ag film thicknesses were determined by replacing the sample with a thickness monitor and calibrating as a function of the energy supplied to the evaporator.

Clean films had a threshold of 4.3 eV. The dosant used to reduce the work function is an organic molecule: 4-picoline (4-methyl pyridine). This molecule has a dipole moment of 2.7 D, a lone-pair orbital on the N, and desorbs from Ag at about room temperature.⁷ The 4-picoline is introduced into the chamber through a UHV leak valve, and is directed at the Ag surface. Pressure rises can be controlled quite well, with a typical dosing

pressure being 1.5×10^{-9} Torr. The lowest threshold observed with adsorbate was near 2.6 eV.

For the laser light, two measurements are of interest. One of these is the reflection signal from the film. The reflection signal is first measured by a photodiode whose output is passed onto a gated amplifier which takes the pulsed reflection signal and returns a dc signal. The dc signal is measured by a Keithley voltmeter. Because of the Al reflecting film on the prism the measured quantity is actually the square of the reflectance.¹²

The other measurement of interest is the photoemission signal. A preamplifier is used to amplify the signal from the collection grid which is biased to +50 V. The output of the preamplifier goes to the gated amplifier. Again a dc signal is the output measured by the Keithley.

A Xe lamp and SPEX monochromator were also used for work-function measurements. The monochromator contributes a spread of about 5 deg to the angular scans of $R(\vartheta)$ and $P(\vartheta)$. The beam as defined by the exit slit of the monochromator is spatially wider than the laser beam. Thus there is a wider range of incident angles on the prism and on the Ag film. Therefore, despite the spectral purity of the monochromator light, the photoyield in the angular scans is not a sharp function of angle as may be seen below.

Electrons liberated by the light are collected at a grid biased to +30 V. The current is measured by an electrometer for selected wavelengths during a wavelength scan. The dynamic range for photocurrent measurements is 10^5 . Wavelength steps of 20 Å are taken between each photoemission data point. Angular scans have a resolution of 0.1 deg and energy scans have a resolution of 0.02 eV. The intersection between noise current (near 1.0×10^{-13} A) and the photocurrent above noise is defined to be the work function of the film.⁷ Note that we cannot make the usual definition of threshold from a Fowler model because of the strong peaks (see below).

An Apple Mac II is used for all data acquisition and storage. National Instrument's LabVIEW software and appropriate hardware are used to control the various instruments over either IEEE-488 or RS-232 protocols.

III. RESULTS AND DISCUSSION

Our measurements of $R(\vartheta, E)$ and $P(\vartheta, E)$ cover the angular range from about 40 to 70 deg for illumination through the prism (ATR configuration) and directly onto the adsorbate-covered Ag film. These angles include total internal reflection at the critical angle, $\vartheta_c \approx 43^\circ$, as well as excitation of SPP and similar modes at angles we label ϑ_r . The photon energy range is from about 2 to 5 eV. This range includes the Ag plasmons at 3.65 and 3.80 eV as well as the photoemission thresholds for bare Ag at 4.3 eV and adsorbate-covered Ag near 2.6 eV. The dielectric constants for calculations were taken from data of Winsemius *et al.*¹⁴ at 90 K, through the present data were taken at 150 K; dielectric constants measured at room temperature^{13,14} lack the strong minimum in ϵ_2 found at low temperatures.

$P(\vartheta)$ is essentially constant in the case of direct illumination. So only the ATR results will be discussed when angle is the variable.

A. Angular response in the ATR configuration

There are three different energy regimes for illumination through the prism and the angular response differs in each, so they will be discussed separately.

The first regime is that of the conventional SPP excitation at energies below 3.6 eV that has been discussed by Raether.¹ Light passing through the prism excites a surface plasmon and the plasmon may decay into a photoelectron. In this energy range we have data for both laser light and also a less-well collimated beam from the SPEX

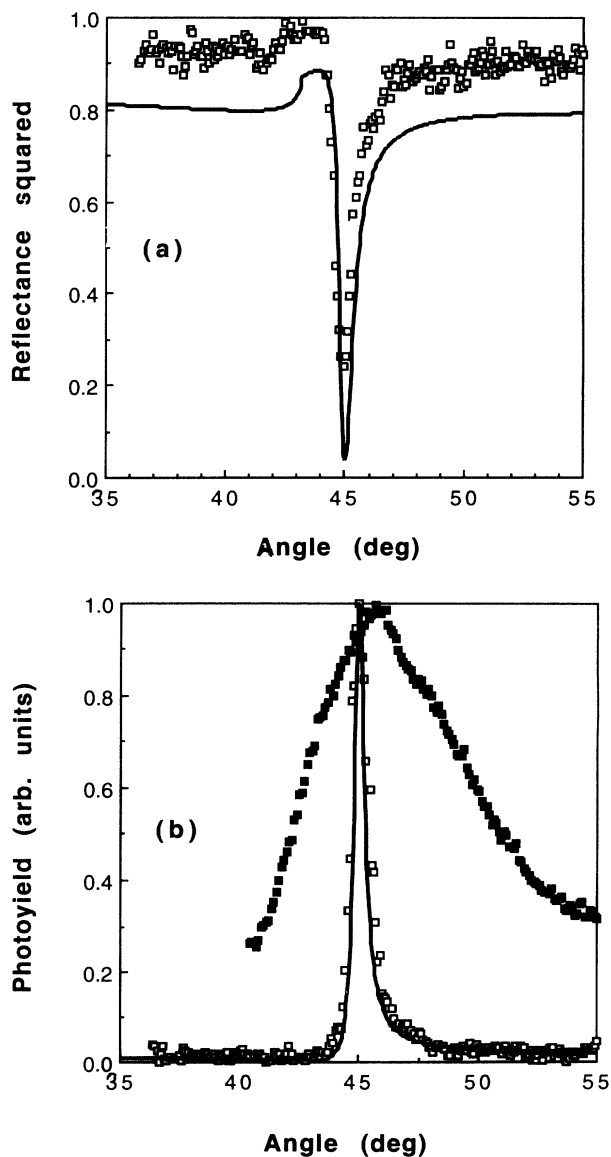


FIG. 1. (a) The square of the reflectance (Ref. 12) in the ATR configuration, open squares, together with reflectance calculated with a dielectric constant $\epsilon_1 = -16.0$ and $\epsilon_2 = 1.5$, solid line. (b) $P(\vartheta)$ measured simultaneously with $R(\vartheta)$ using the laser, open squares, and also measured separately with a beam from the SPEX monochromator at 2.47 eV, solid squares. The solid line shows a calculated yield.

monochromator. The laser data reveal details obscured by the spread of the monochromator. As only the monochromator data are available at higher energies, we show both in this range.

Figure 1(a) shows $R(\vartheta)$ at 2.13 eV in the SPP range below 3.6 eV. The data have been normalized to 100% at the critical angle. The resonance at 45 deg is just that expected from literature¹³ values of the Ag dielectric constant, $\epsilon(\omega)$, as may be seen from the quality of the superimposed calculated curve. The value of $R(\vartheta_r)$ is higher than predicted because of a slight misalignment of the direct and reflected beams.

The photoyield $P(\vartheta)$ also peaks at the angle of the plasmon excitation as may be seen in Fig. 1(b) for laser light. Figure 1(b) also shows the photoemission calculated from Pepper's model¹¹ using optical constants taken at 90 K by Winsemius *et al.*¹⁴ As there are no adjustable parameters, except for normalization of the photocurrent, the agreement is quite good. The monochromator data in Fig. 1(b) was taken at 2.47 eV and is included to demonstrate the width introduced to the angular scans by the monochromator.

The second regime is between the surface plasmon at 3.6 eV and the bulk plasmon at 3.9 eV. The maxima in $P(\vartheta)$ are very broad and there is no recognizable resonance in the reflectances. The angle for maximum photoemission ϑ_r decreases with increasing photon energy. Near 3.65 eV there is a large surface contribution to photoemission caused by the roughness of the film.¹⁶ The surface term is about the same size as the volume term and can be separated to some extent as it does not shift with angle. Figure 2 shows an example of the calculated and measured photoemission in this range. The calculated curve has been shifted vertically to coincide with the measurements and facilitate comparison of peak location

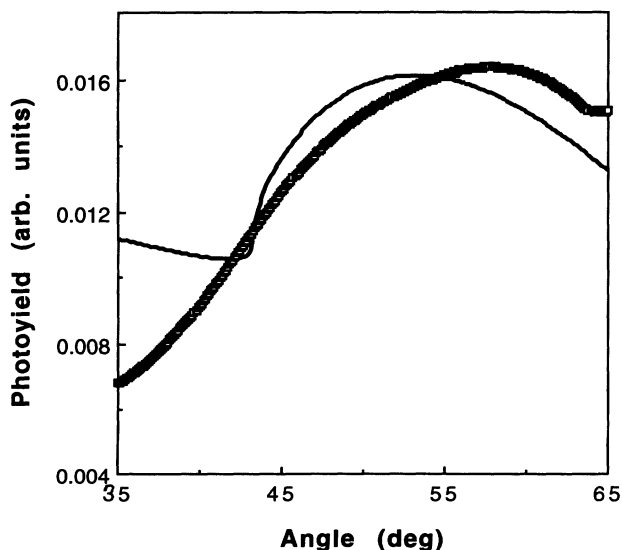


FIG. 2. Squares show the measured $P(\vartheta)$ and the solid line represents the calculated $P(\vartheta)$ at 3.76 eV, in the energy range between the surface and bulk plasmon resonances.

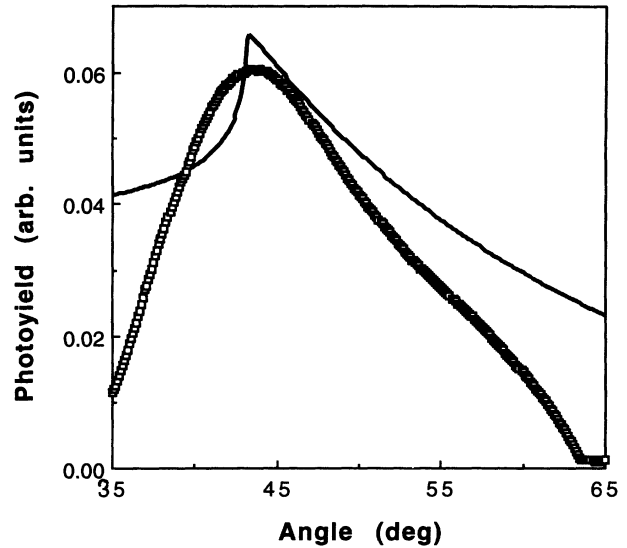


FIG. 3. Measured and calculated $P(\vartheta)$ at 3.90 eV, in the energy range above the bulk plasmon resonance, with the same notation as in Fig. 2.

and width. The large volume photoyield occurs in part because the Ag loss term $\epsilon_2(\omega)$ is large.^{1,15} Note that the 5 deg instrumental width is sufficient to obscure the calculated break in the yield at ϑ_c .

The third range lies above the bulk plasmon at 3.80 eV. The $\epsilon_2(\omega)$ for Ag is still large so that the peaks in $P(\vartheta)$ are broad, but the peak angle is an increasing function of the photon energy, as it is below 3.6 eV. There is much less influence of the surface yield. The peak angle does not correspond to a Brewster resonance¹⁵ as reported by Callcott and Arakawa.² Yet, as may be seen in Fig. 3, the

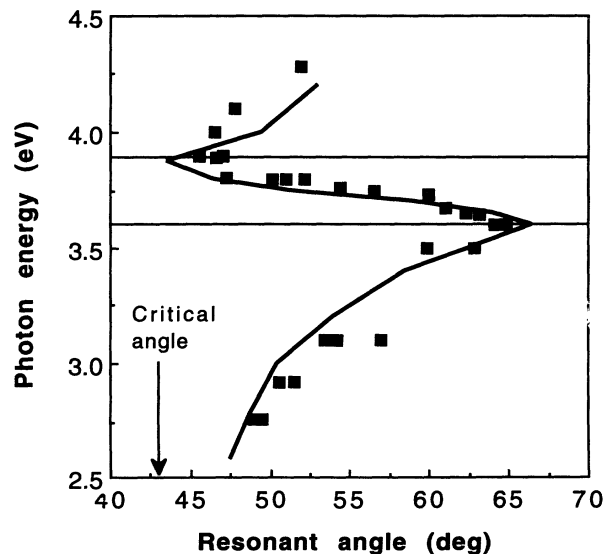


FIG. 4. Experimental and calculated dispersion relation $E(\vartheta)$.

location and shape (as smeared by the spread of the beam) of the peak are fairly well represented by Pepper's model.

Finally in Fig. 4, we present the dispersion relation $E(\vartheta)$ determined from maxima in $R(\vartheta)$ and $P(\vartheta)$ such as depicted in Fig. 1 and also $P(\vartheta)$ data obtained at higher energies as shown in Figs. 2 and 3. In the SPP regime below 3.6 eV, reflectance minima and photoemission maxima coincide so that the dispersion curves are the same. Above 3.6 eV there are no reflectance minima so we use $P(\vartheta)$ data. Errors in fixing the peak location, even in broad curves such as Figs. 2 and 3, are generally within 1 deg. Our observed dispersion curve agrees well with that calculated from Pepper's model, as also shown in Fig. 4.

B. Photoemission spectra in the ATR configuration

The curves presented in Figs. 1–3 do not fully reveal trends with energy. The measured magnitude of the photoyield in the intermediate regime between 3.4 and 3.8 eV is substantially greater, relative to the yield outside that range, than is predicted by Pepper's calculation of the volume photoyield.

Peaks and minima in $P(E)$ for ϑ fixed at 55 deg will be discussed first. $P(E)$ obtained with illumination *through* the prism has three peaks, Fig. 5(a). The energy of the lowest peak depends on the angle of incidence. In contrast the middle peak at 3.65 eV [only partly resolved in Fig. 5(a)] and the highest-energy peak at 3.95 eV have no dependence upon angle of incidence.

SPP coupling through the attenuated-total-reflection mechanism is responsible for the low-energy peak. As the angle of incidence varies, the photon energy needed for coupling varies according to the well-known dispersion relation¹ already shown in Fig. 4.

Surface roughness coupling of light to the SPP is responsible for the photocurrent peak at 3.65 eV. There is no angular dependence with such coupling.¹⁶

For prism illumination, Fig. 5(a), the photons have to go through the Ag film to reach the vacuum interface. With increased absorption above 4 eV, the field strength near the vacuum interface is decreased leading to reduced photocurrent. As we shall see there is a pronounced difference in $P(E)$ above 4.0 eV for photocurrent induced by illumination incident directly and through the prism.

Figure 5(a) also contains a comparison of predicted and observed $P(E)$ for light coming through the prism. The agreement is generally good at high energies. The broad monochromator beam causes the maximum observed near 3.45 eV to be a superposition of yields for a range of incident angles [see Fig. 1(b)]. Pepper's model produces a peak at 3.3 eV with light incident only at 55 deg, as shown; addition of a 61 deg contribution shifts the peak to 3.4 eV.

The model predicts a minimum resulting from the minimum in the Ag absorption (ϵ_2) at 3.86 eV at the low temperatures of the experiment. (That minimum is absent at room temperature.^{13,14}) The experimental minimum is slightly lower at 3.80 eV. For energies above 4 eV light is absorbed too far from the exposed surface

for photoelectrons to escape and the yield is predicted to decline just as observed.

It is clear from Fig. 5(a) that the model totally misses the enormous yield at 3.65 eV. This flaw exists for direct illumination of the Ag film and also for illumination through the prism. We attribute this discrepancy to the presence of a large *surface* photoyield in the neighborhood of the SPP resonance and only a *volume* photoyield at other, higher energies. Pepper only provides a model for volume photoemission. The separation of surface and volume contributions to the photoyield is not a straightforward process.^{5,17}

The features of Fig. 5 are "exposed" as the addition of

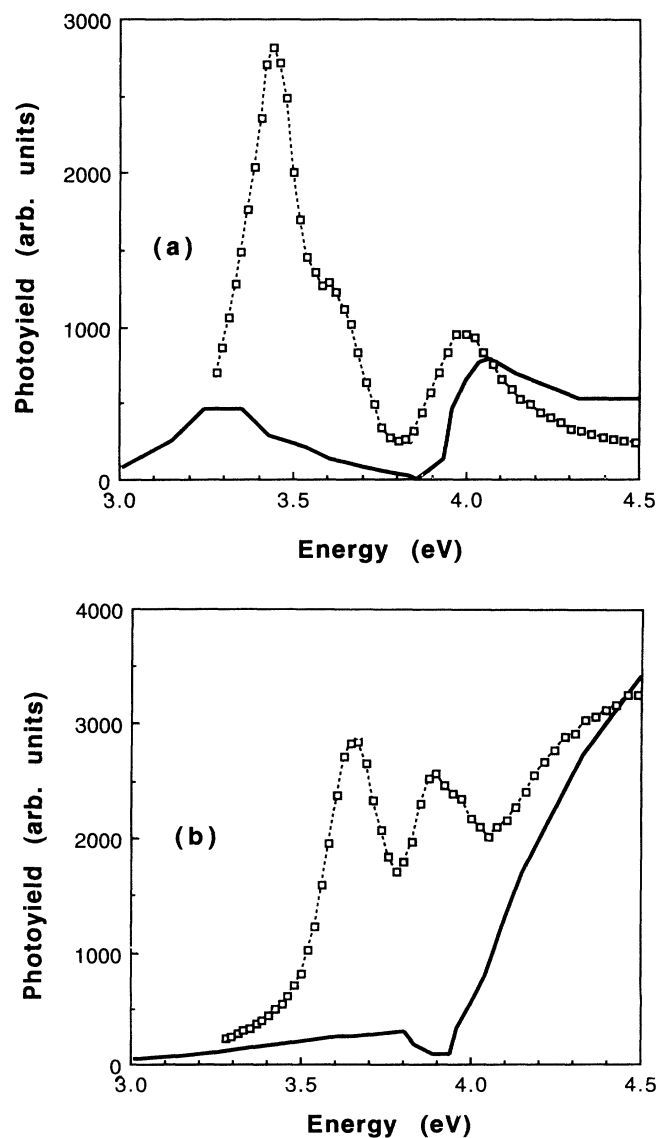


FIG. 5. (a) Measured and calculated $P(E)$ for a 55 deg angle of incidence through the prism (ATR configuration). (b) Measured and calculated $P(E)$ for a 55 deg angle of incidence with direct illumination of the Ag film. The threshold (not shown) is 2.65 eV.

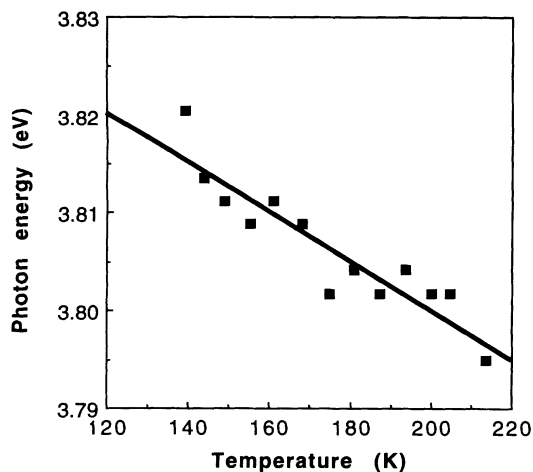


FIG. 6. A plot of the energy of photoemission minima such as shown in Fig. 5(a) near 3.8 eV vs temperature is shown. Light is incident upon the Ag film through the prism. The diagonal line is a linear fit to the points with a slope of -2.5×10^{-4} eV/K.

adsorbate reduces the photothreshold from the 4.2-eV characteristic of clean Ag to the limiting value of 2.6 eV with a monolayer. The positions of the peaks and valleys change little with coverage. For the ATR configuration and for a monolayer of adsorbate, we have followed the feature lying at highest energy, the minimum in $P(E)$ near 3.80 eV, with temperature, see Fig. 6. The minimum in $P(E)$ shifts with temperature with a slope of about $-2.5 \pm 0.5 \times 10^{-4}$ eV/K. Pepper's model¹¹ predicts a minimum at 3.86 eV associated with the low value of ϵ_2 at that energy, as already noted. The energy of the Ag absorption edge just above the minimum shifts at the rate of -6.5×10^{-4} eV/K according to Winsemius *et al.*¹⁴ Shifts in the bulk plasmon energy detected in the past by experiments on electron energy loss,¹⁸ thin Ag film light transmission,¹⁹ and reradiation of absorbed light,^{20,21} are similar to our value. Rocca, Moresco, and Vlabusa²² found a shift of the surface plasmon of -9×10^{-5} eV/K. Calculations^{14,18,20} show that thermal expansion of the Ag film is not sufficient to account for the change with temperature of the bulk plasmon energy. The complexities of the Ag band structure responsible for the plasmon being at such a low energy make a simple explanation of the temperature effect difficult.

C. Photoemission spectra with direct illumination

When photoemission is produced by *direct* illumination of the adsorbate-covered Ag film there are only two peaks in $P(E)$, at 3.65 and 3.88 eV, Fig. 5(b). Minima are at 3.80 and 4.07 eV. Surface roughness-induced coupling^{7,16} of light to the SPP causes the photocurrent peak at 3.65 eV, just as with the ATR experiment. Also just as in the ATR, Pepper's model is not designed to include

yields generated by surface roughness and cannot predict the peak at 3.65 eV for direct illumination.

The Pepper model predicts a gentle rise of P with increasing energy until a small peak is reached at the bulk plasmon followed by a minimum near the energy of the minimum in ϵ_2 . The model predicts a smoothly rising yield at all energies above 3.9 eV without any structure. The observed peak in $P(E)$ near 3.9 eV and the minimum at 4.1 eV occur for all of our experiments at all adsorbate coverages sufficient to lower the work function and expose the peak at 3.65 eV, and for all angles of incidence. Similar peaks and valleys in this energy range are found if one compares the transmission of a thin Ag film for p -polarized light to the photoemission curve. Hincelin⁵ has reported a "spurious signal" at 3.85 eV similar to what we show in Fig. 5(b).

IV. SUMMARY

In summary, we are able to obtain an understanding of most of the features found in our measurements of reflectance $R(\vartheta, E)$ and photoemission $P(\vartheta, E)$ by comparing $R(\vartheta, E)$ and $P(\vartheta, E)$ with the predictions of Pepper's model and by using the low-temperature dielectric constants measured by Winsemius *et al.* First, with illumination through the prism, the peaks at energies below 3.6 eV are the well-known surface plasmon polariton resonance and occur at energies dependent on the angle of incidence. Second, the dispersion curve $E(\vartheta)$ determined from maxima in $P(\vartheta)$ is consistent with Pepper's volume photoyield model. Third, the minimum observed at 3.80 eV with both prism and direct illumination is the consequence of the very low values of ϵ_2 near this energy that occur only at low temperatures.¹⁴ Fourth, the large yield found at 3.65 eV is the consequence of coupling to surface plasmons allowed by the rough surfaces of the thin films and is not covered by Pepper's model.

Features above 3.9 eV are less well understood, particularly the minimum at 4.1 eV in $P(E)$ with direct illumination of the Ag film. Absorption in Ag rises very rapidly above 3.9 eV at low temperatures.¹⁴ Though this rise is shown, by Pepper's model, to cause the rising $P(E)$ in this energy range for prism illumination, there is no hint of an effect one way or the other in the calculations for direct illumination.

Pepper's model does show that increased absorption reduces the photoyield above 4 eV when light passes through the Ag film in the ATR configuration.

ACKNOWLEDGMENTS

This work has been supported in part by the R. A. Welch Foundation of Texas and by the Texas Advanced Research Program. We appreciate informative discussions with P. R. Antoniewicz, J. C. Villagrán, and H.-T. Chou.

- ¹H. Raether, *Surface Plasmons on Smooth and Rough Surfaces and On Gratings* (Springer-Verlag, Berlin, 1988).
- ²T. A. Callcott and E. T. Arakawa, *Phys. Rev. B* **11**, 2750 (1975).
- ³T. Tsang, T. Srinivasan-Rao, and J. Fischer, *Phys. Rev. B* **43**, 8870 (1991).
- ⁴H.-T. Chou, J. C. Villagrán, and J. C. Thompson, *Phys. Rev. B* **44**, 3359 (1991).
- ⁵G. Hincelin, *Phys. Rev. B* **24**, 787 (1981).
- ⁶T. López-Ríos and G. Hincelin, *Phys. Rev. B* **38**, 3561 (1988).
- ⁷C.-W. Kim, J. C. Villagrán, U. Even, and J. C. Thompson, *J. Chem. Phys.* **94**, 3974 (1991).
- ⁸J. C. Quail and H. J. Simon, *Phys. Rev. B* **31**, 4900 (1985).
- ⁹J. T. Stuckless and M. Moskovits, *Phys. Rev. B* **40**, 9997 (1989).
- ¹⁰H. W. Rudolf and W. Steinmann, *Phys. Lett.* **61A**, 471 (1977).
- ¹¹S. V. Pepper, *J. Opt. Soc. Am.* **60**, 805 (1970).
- ¹²J. C. Villagrán and J. C. Thompson, *Rev. Sci. Instrum.* **60**, 1201 (1989).
- ¹³E. D. Palik, *Optical Constants of Solids* (Academic, New York, 1985), Vol. 1.
- ¹⁴P. Winsemius, F. F. van Kampen, H. P. Lengkeek, and C. G. van Went, *J. Phys. F* **6**, 1583 (1976).
- ¹⁵E. Burstein, in *Polaritons*, edited by E. Burstein and F. DeMartini (Pergamon, New York, 1974).
- ¹⁶A. J. Braundmier and E. T. Arakawa, *J. Phys. Chem. Solids* **35**, 517 (1974).
- ¹⁷G. Chabrier, J. P. Goudonnet, and P. J. Vernier, *Phys. Rev. B* **13**, 4396 (1976).
- ¹⁸D. Schulz and M. Zurheide, *Z. Phys.* **211**, 165 (1968).
- ¹⁹J. Brambring and H. Raether, *Z. Phys.* **199**, 118 (1967).
- ²⁰E. T. Arakawa, N. O. Davis, and R. D. Birkhoff, *Phys. Rev.* **135**, A224 (1964).
- ²¹J. Daniels, *Z. Phys.* **203**, 235 (1967).
- ²²M. Rocca, F. Moresco, and U. Vlabusa, *Phys. Rev. B* **45**, 1399 (1992).